

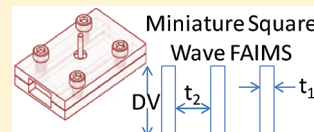
Comparison of Rectangular and Bisinusoidal Waveforms in a Miniature Planar High-Field Asymmetric Waveform Ion Mobility Spectrometer

Marilyn Prieto,[†] Chia-Wei Tsai,[†] Said Boumsellek,[‡] Robert Ferran,[‡] Ilya Kaminsky,[‡] Scott Harris,[‡] and Richard A. Yost^{*,†}

[†]Department of Chemistry, University of Florida, P.O. Box 117200, Gainesville, Florida 32611, United States

[‡]Implant Sciences, 11558 Sorrento Valley Road, San Diego, California 92121, United States

ABSTRACT: High-field asymmetric waveform ion mobility spectrometry (FAIMS) separates ions by utilizing the mobility differences of ions at high and low fields. The shape of the waveform is one of the essential features affecting the resolution, transmission, and separation of FAIMS. Due to practical circuitry advantages, sinusoidal asymmetric waveforms are typically used in FAIMS, whereas theoretical studies indicate that square asymmetric waveforms improve ion separation, resolution, and sensitivity. Results from FAIMS using square and sinusoidal waveforms are presented, and effects of the waveforms on ion separation are discussed. A FAIMS system interfaced with a quadrupole ion trap mass spectrometer was used in this study. FAIMS spectra were generated by scanning the compensation voltage (CV) while operating the mass spectrometer in total ion mode. The identification of ions was accomplished through mass spectra acquired at fixed values of ions' CVs. Square waveform evaluation was done by acquiring data at three frequencies and six duty cycles of the square waveform generator. The performance of FAIMS using square and sinusoidal waveforms at 250, 333, and 500 kHz frequencies was compared, and trends were identified. For all frequencies, the best response of FAIMS was achieved at the lower amplitudes and under the lower duty cycles of the square waveform generator. The separation of FAIMS was better at the higher frequencies. These results demonstrate the potential to incorporate square-wave FAIMS into the design of a miniature device for detection of explosives in the field. SIMION version 8.0, the ion trajectory modeling program, was utilized to optimize the performance of the miniature FAIMS cell and to validate experimental results.



Overview. High-field asymmetric waveform ion mobility spectrometry, or FAIMS, operates at atmospheric pressure to separate and detect gas-phase ions, as first described in detail by Buryakov et al.¹ At high fields ($\sim 10\,000$ V/cm), ion mobilities become dependent on the applied field and are represented by K_h , a nonconstant high-field mobility term. Variations in K_h from the low-field K , and the compound-dependence of that variation, are what give FAIMS its separation power. FAIMS utilizes a combination of alternating current (ac) and direct current (dc) voltages to transmit ions of interest and filter out other ions, thus decreasing the chemical noise and improving specificity. FAIMS can reduce false positives, since two different compounds having the same low-field mobility can often be distinguished in a high-field environment.² The fundamental processes of FAIMS have been described elsewhere.^{3–5}

The most commonly used asymmetric waveform, described by $V(t)$ in eq 1, consists of a high-voltage component [also referred to as V_1 or dispersion voltage (DV)] which lasts for a short period of time (t_1) relative to a longer lasting (t_2) low-voltage component (V_2) of opposite polarity. Most FAIMS work up to date has employed a sinusoidal wave, plus its phase-shifted second harmonic, as shown in eq 1, where ω is the frequency in rad/s. The waveform is constructed so that the voltage–time product applied to the electrode is equal to zero, as displayed in eq 2 and Figure 1.

$$V(t) = (0.61)V_1 \sin(\omega t) + (0.39)V_1 \sin(2\omega t - \pi/2) \quad (1)$$

$$V_1t_1 + V_2t_2 = 0 \quad (2)$$

At high electric fields, the application of this waveform will cause an ion to experience a net drift toward one of the electrodes. Ions passing between the electrodes encounter this displacement because the ion's mobility during the high-voltage component (K_h) is different than that from the low-voltage mobility (K). In other words, the ion will move a different distance during the high-voltage portion than during the low-voltage portion. This ion will continue to migrate toward one of the electrodes and subsequently be lost unless a dc compensation voltage (CV) is applied to offset the drift. The CV values required to offset the drift of different ions will be different if the K_h/K ratios of the ions are different. Thus, a mixture of compounds can be successfully separated by scanning the CV, allowing each compound to transmit at its characteristic CV, creating a CV spectrum.

Rectangular Waveform. Even though most FAIMS experiments have made use of the sum-of-sines waveform, theoretical studies have suggested that a rectangular (also termed square) waveform (as shown in Figure 1b) would be ideal for FAIMS analyses.^{6–8} Analytical considerations show that square waveforms may improve ion separation efficiency, resolution, and/or sensitivity as compared to sinusoidal waveforms.^{8–11} Unfortunately, practical use of electronics that deliver square pulses for driving differential ion mobility separations has been hindered due to the excessive power load imposed by the system.⁶

Received: April 12, 2011

Accepted: October 21, 2011

Published: October 21, 2011

Intuitively, the use of an asymmetric square waveform for FAIMS would seem to maximize the differences during the high- and low-field portions of the electric field. These high to low periods of the waveform permit an ion to experience a maximum of unequal voltages maximizing the CV. In previous studies, there have been concerns that the time it takes an ion to respond to the idealized asymmetric square waveform and reach “steady state”, or terminal, drift velocity might be sufficiently long to introduce error due to the transient electric field.⁴ Lin et al.¹² showed that, to the first order, this can be neglected if the time for reaching terminal velocity is small relative to the total drift time. Since the estimated time necessary to reach this velocity in a transient electric field is in the picosecond range and the drift time is in the millisecond range, this factor can be ignored.

Because FAIMS has continuous ion separation capabilities, it is attractive to use in conjunction with a mass spectrometer. This union can be utilized to offer orthogonal detection methods, one separating ions according to their mobilities and the other separating ions according to their mass-to-charge ratios. In this article, we describe how the independent control (frequency, amplitude, and duty cycle) of a square waveform can help in the characterization of FAIMS transmission, resolution, and

separation and in comparison with the results obtained while using a sum-of-sines waveform. Previous experiments performed by Papanastasiou et al. have shown the duty cycle to have a strong influence on ion separation with planar electrodes.^{6,13} It should be noted that our research was done independently and was carried out without knowledge of the work being performed by Eiceman’s team.⁶ In this paper we describe a miniature FAIMS cell, powered by a digitally driven circuit producing a square waveform, and compare it with the same cell powered by an analog sum-of-sines waveform. A comparison of separation and sensitivity is performed over the overlapping range provided by the waveform generators. SIMION 8¹⁴ modeling is used to validate experimental results. A miniature FAIMS cell, powered by a computer-controlled square waveform, could be an attractive design for detecting explosives in the field.

■ EXPERIMENTAL SECTION

The traditional sinusoidal waveform was created by an Ionalytics GPI 1000 FAIMS system α prototype waveform generator which runs with a 2:1 ratio (33% duty cycle) at a frequency of 750 kHz. This waveform was applied to one of the plates, and a reference lead was applied to the other plate. Each individual component sine waveform was capacitance-tuned for the electrodes and added together to produce a waveform such as that shown in Figure 1a. The α waveform generator is designed to produce a waveform across a certain load. The generator is unable to produce this waveform if there is not enough capacitance; thus, the FAIMS cell acts as a capacitor that must be tuned. The full range of DV for the Ionalytics α prototype is ± 300 to ± 4000 V; the range utilized for this research was from ± 300 to ± 350 V. Data were processed using the mass spectrometer instrument software (described below).

The square waveform generator used in these studies was first described by Tsai et al.¹⁵ and constructed by Implant Sciences Corporation (patent application no. 13/066,894); a schematic is shown in Figure 2c. Our square-wave driver is not a laboratory-type power supply but rather a miniature, low-power, low-cost circuit intended to be integrated into a hand-held product. It uses

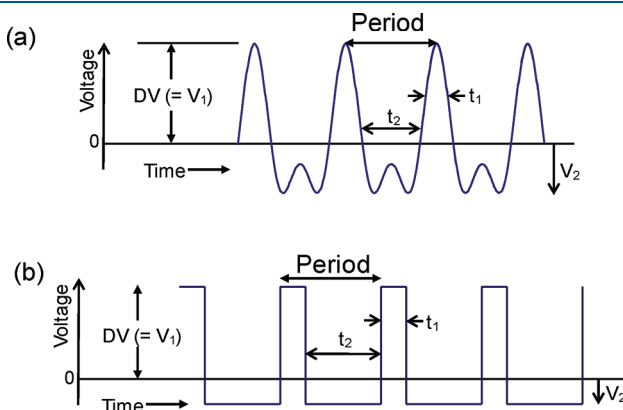


Figure 1. Generic schematic of (a) an asymmetric sum-of-sines waveform and (b) a square waveform.

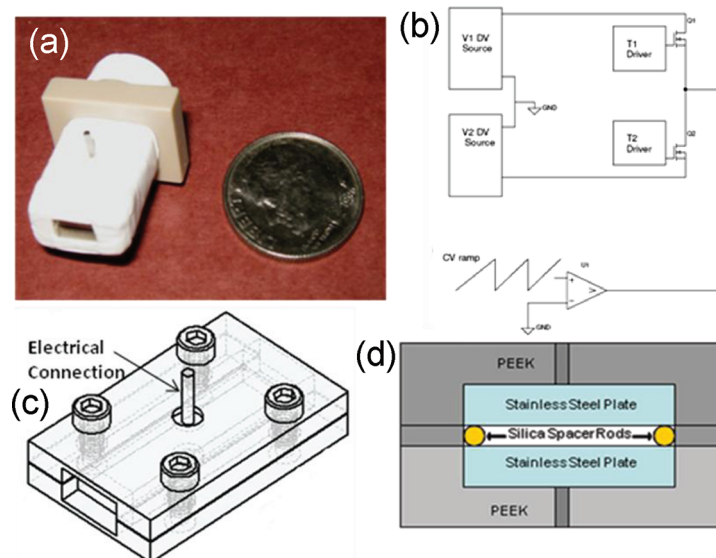


Figure 2. Picture (a), square-wave generator circuit diagram (b), schematic (c), and cross view of planar FAIMS cell (d).

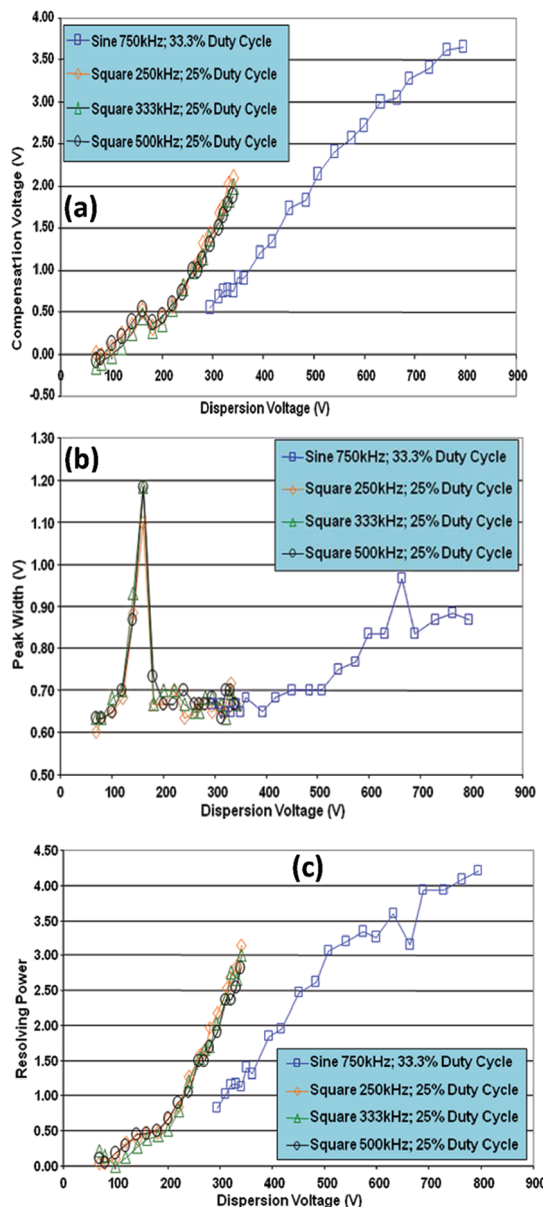


Figure 3. Graphs displaying behavior of CV (a), peak width (b), and resolving power (c) as a function of DV.

miniature EMCO power supplies and high-voltage breakdown transistors.

The method consists of using direct transistor switching at high speed and at reasonable power losses. The choice of high-voltage (>1000 V) fast transistors (FETs) with low output capacitance is limited. On one hand, the 1500 V transistors are very slow, and on the other, the 1200 V FETs have large output capacitances making the switching at high speed power-consuming. The circuits use 800 V transistors or FETs (which are fast and have low output capacitances) in series to carry very high voltages. The main source of power losses in this circuit with low current is the low inductance charging and discharging of output capacitance (C_{oss}) of the FETs themselves. The low C_{oss} and high-voltage FETs are designed for low-power applications, packaged in TO-92, and cannot handle losses higher than 1 W per FET. To solve this problem they have assembled several transistors in parallel to limit the current through each.

The actual drive waveforms were generated by their embedded computer. Two switching waveforms were used, one to drive the positive voltage and one for the negative voltage. These waveforms provided for adjustments to account for the circuit peculiarities and to provide the necessary dead time to ensure low-power switching. Computer simulations were carried out to optimize the switching scheme and hence obtain a waveform at a total power of only 0.5 W. The computer, if desired, can continuously adjust the time portion shape of the waveform. Their circuit includes the ability to set the compensation voltage to be applied to the opposite electrode of the FAIMS and, therefore, use an adjustable lower voltage time (t_2) instead of a compensation voltage hence providing large savings in circuitry and power. The circuit has been described extensively in a patent application called "Chemical Analysis using Hyphenated Low and High Field Ion Mobility" assigned to Implant Sciences.

The square waveform generator can provide positive DV values from +50 to +750 V. Three different frequencies (250, 333, 500 kHz) and six different duty cycles [25%, 30%, 33.3%, 35%, 40%, and 45%, defined as $t_1/(t_1 + t_2)$] were evaluated on this waveform generator unless otherwise noted. All experiments employed a CV separation over a 10 V range at a scan rate of 5 V/min. Square waveform was controlled using the instrument software interface (DMS interface version 0.25) created by Implant Sciences.

The planar geometry FAIMS cell, as shown in Figure 2, parts a, c, and d, was designed by the University of Florida Chemistry Department Machine Shop and consists of two parallel stainless steel plates (5 mm wide, 15 mm long, 1 mm thick) encased and recessed in a poly(aryl ether ether ketone) (PEEK) support (8 mm wide, 18 mm long, 3 mm thick) that provides mechanical stability and electrical insulation. Electrical connections to the individual plates were made via posts spot-welded to the plates through holes in the PEEK support. The gap within the FAIMS cell (0.38 mm) was maintained by fused-silica capillaries as shown in Figure 2d. The top and bottom plates were then secured to each other through the PEEK with four screws to ensure mechanical stability and alignment.

The FAIMS cell was interfaced directly to the heated capillary inlet of an LCQ (Thermo Scientific) quadrupole ion trap mass spectrometer (QITMS) with the aid of a home-built end-cap connector piece. All experiments were performed utilizing this commercial benchtop MS. The end-cap piece was made of PEEK and is displayed in Figure 2a (top left). The end-cap piece and FAIMS cell were mounted in Teflon housing to ensure no ion loss occurred between these connections. No curtain plate or curtain gas was used and no attempt to perform additional ion desolvation was made. Conventional atmospheric pressure chemical ionization (APCI) was employed to produce gas-phase ions. Nitrogen was used as the nebulizing (sheath) and auxiliary gases. Sheath gas flowed at 20 arbitrary units, and auxiliary gas was at 8 arbitrary units. The FAIMS carrier gas used was ambient air. APCI and heated capillary temperatures were held at 75 °C with a current of 3.25 μA. Analyte samples were infused with a 500 μL Hamilton syringe at 15 μL/min. Solutions were injected directly via the syringe pump of the LCQ. Data acquisitions were performed using full scan mode (50–500 m/z) with a maximum injection time of 100 ms for automatic gain control (AGC). Data were processed using the instrument software interface (Xcalibur version 1.4 SR1).

In this research, a common explosive, 2,4,6-trinitrotoluene (TNT), was utilized. This explosive was provided by Dr. Jehuda Yinon of

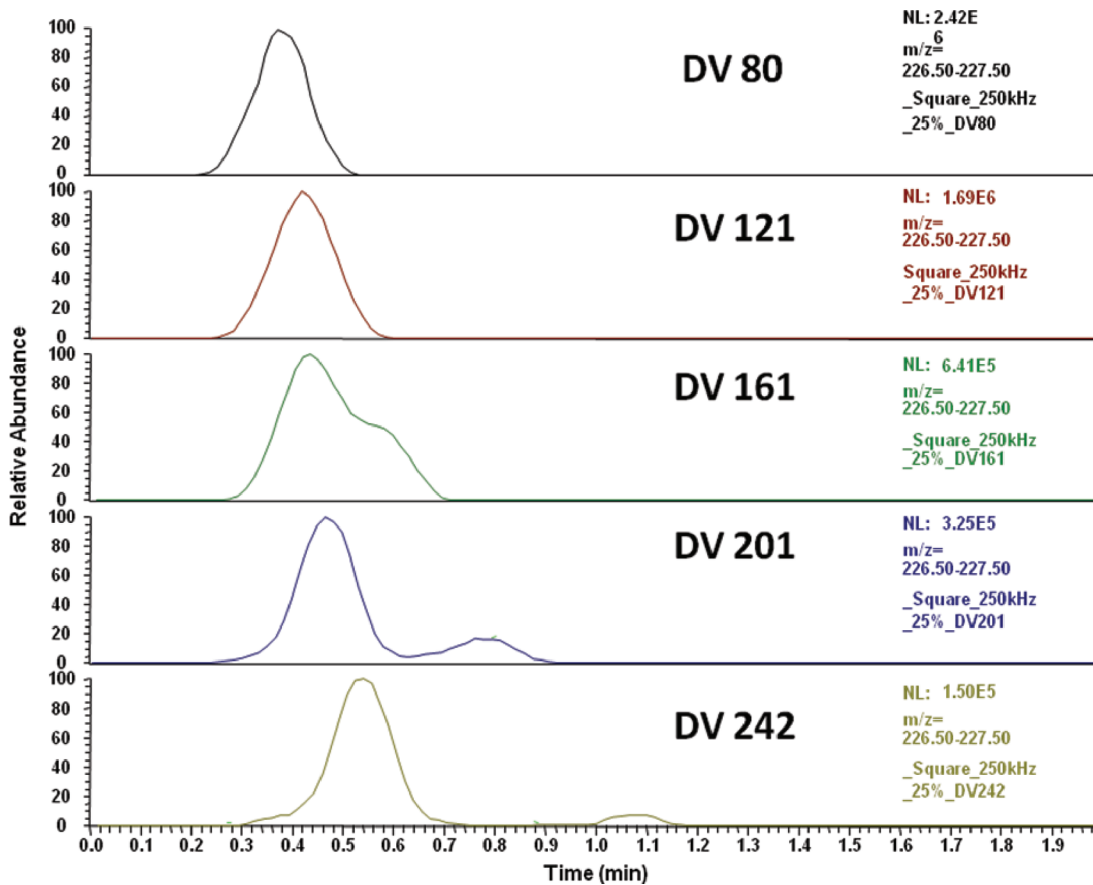


Figure 4. CV separation of m/z 227 ions. CV scanned from -2 to 8 V over 2 min.

the Weizmann Institute of Science and was obtained from the Analytical Laboratory of the Israeli Police Headquarters. Negative ion mode was employed with APCI. The explosive solution was diluted in a solvent mixture consisting of 65% methanol and 35% deionized water. Utilizing a combination of methanol and water as a solvent allows the use of lower vaporizer temperatures than water alone; the low vaporizer temperature helps avoid the degradation of fragile explosive analytes. In this research, all solutions were diluted to a concentration of 10 ppm unless otherwise noted.

SIMION 8, the ion trajectory modeling program,¹⁴ was utilized in an effort to optimize the performance of the miniature FAIMS cell and validate experimental results. These simulations were first described by Tsai et al.¹⁵ The influences of pneumatic and electrostatic forces at atmospheric pressure were shown. The variables used in this investigation include gas flow, DV, CV, analytical gap (spacing between the plates), frequency of the asymmetric waveform, its shape (sinusoidal vs square), and its duty cycle. The potential array of the FAIMS analyzer consisted of parallel plates (5 mm wide, 15 mm long, and separated by a gap, $G = 0.38$ mm). The Statistical Diffusion Simulation⁸ (SDS) user program was invoked to model ion motion at atmospheric pressure. By modeling both diffusional and mobility terms of ions in a neutral gas, the effects of high-pressure collisions are identified. All simulations were performed using TNT, $[M]^-$, ions ($m/z = 227$) for which the low-field and high-field mobilities are known.^{9,17-19,23}

Resolving power (R_p) indicates the ability of the FAIMS cell to resolve a peak at a particular CV.²⁰ R_p is defined as the CV

divided by the peak width at half-maximum (PWHM) as shown in eq 3.

$$R_p = \frac{CV}{PWHM} \quad (3)$$

Here, the duty cycle, d , is defined as

$$d = \frac{t_1}{t_1 + t_2} \quad (4)$$

RESULTS AND DISCUSSION

Influence of DV on CV, Peak Width, and Resolving Power. The performance of the square waveform on planar FAIMS ion separation was investigated. In FAIMS, ions are separated based on the change in their mobility at high versus low electric fields. Thus, theoretically, the higher the field, the better separation is achieved. Generally, the magnitude of the CV increases as the DV increases for low-mass ions (m/z usually below 300). This behavior is observed with both the sum-of-sines and square-wave waveform generators, as displayed in Figure 3a. The plot shows CV as a function of DV for both waveforms with the sine wave at 750 kHz and the square wave at three different frequencies (250, 333, and 500 kHz). The duty cycle for the sine waveform was 33% (not adjustable); a duty cycle of 25% was selected for the square waveform. It is evident that, for both square and sine waves, CV increases with DV, with the square waveform giving higher CV magnitudes within a 300–350 V DV

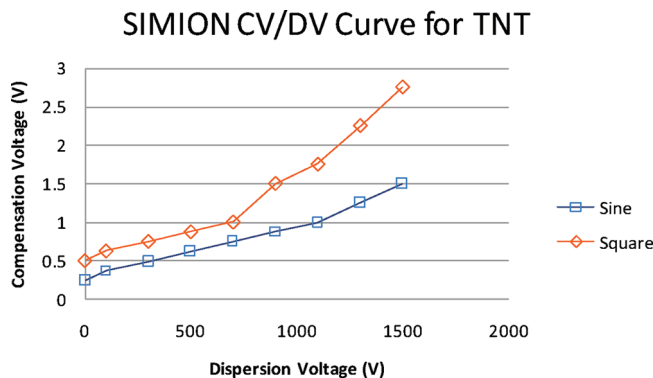


Figure 5. CV versus DV simulation data for the $[M]^-$ ion of TNT.

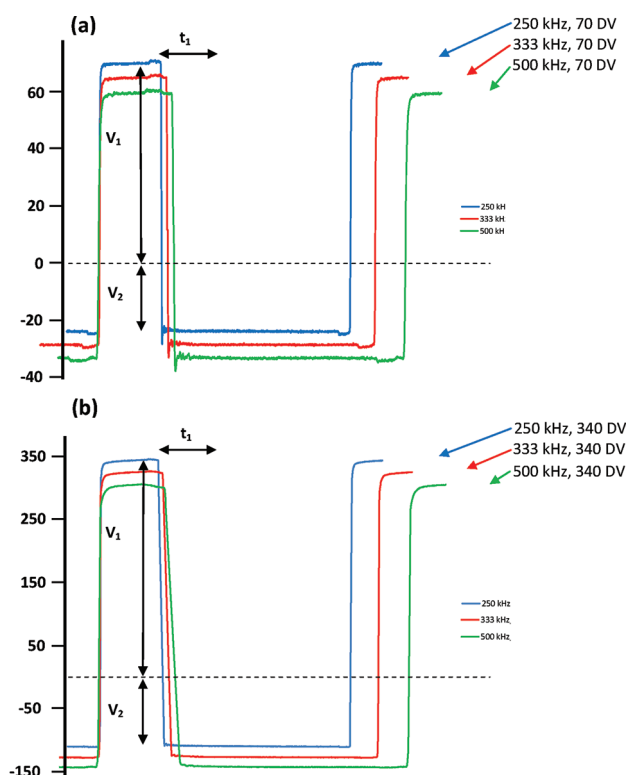


Figure 6. Oscilloscope traces of square waveforms at different frequencies for amplitudes (a) DV 70 and (b) DV 340 where V_1 is the amplitude (DV) and t_1 is the width of the high-voltage pulse. Waveforms are offset for ease of visualization.

range (32–38 Td). The overlapping range was limited to 50 V because peaks above 38 Td were very difficult to detect (due to overheating of the generator), even with heavy averaging of the extracted spectra. This issue is of obvious concern to us, and further work is being performed to extend the usable range of the square waveform generator. The frequency of the square waveform has no significant effect on the CV (figure not shown). Further insight into the behavior of the $[M]^-$ ion in the planar geometry FAIMS cell can be gained by simulation of ion trajectories with SIMION. Figure 5 compares the plots for CV versus DV for both waveforms, over a wider range of DV that can be achieved with our current electronics. Comparing these plots with the experimental data in Figure 3a shows the same trend of higher CV values for the square waveform than for the sine

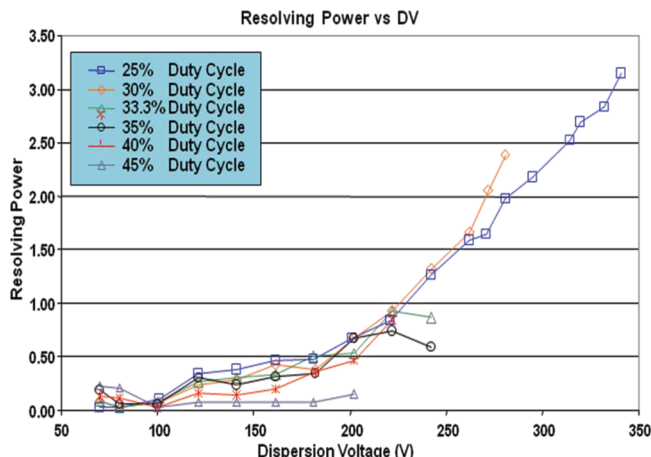


Figure 7. R_p as a function of DV at six different duty cycles.

waveform at the same DV (although only a 1.5× increase, less than the 2.5× increase was observed experimentally). Note that the simulated CV values are generally smaller than those observed experimentally, perhaps because of the increased CV values recently observed in the presence of solvent vapor in the FAIMS cell.²¹

Figure 3b shows that experimental peak widths (full width at half-maximum, PWHM) generally increase as DV increases for both waveforms, although the peak width for the square wave increases only slightly over the available DV range. The dramatic increase in peak width for the square waveforms around DV 150 V (16 Td) and the sine waveform around DV 650 V (70 Td) is due to splitting of the main TNT peak into two peaks. To investigate this further, we took several CV scans at 40 V intervals from 9 to 26 Td, and this is shown in Figure 4. This peak splitting phenomena could be due to an ion with m/z 227, other than TNT, which moves at a faster rate with increasing DV.¹⁶

Figure 3c displays that the R_p increases with DV for both waveforms and higher R_p values are obtained for the square waveform up to 350 DV (38 Td). Even though broader peaks are observed at higher DVs, as shown in Figure 3b, the even greater increase in CV (Figure 3a) results in enhanced R_p .²² The dip observed for the sine waveform around DV 650 V (70 Td) corresponds with the peak splitting seen in Figure 3b.

Influence of Frequency and Duty Cycle on CV, PWHM, and R_p . The square asymmetric waveforms were monitored at different amplitudes and frequencies with a 100 MHz Tektronix TDS 1012B oscilloscope, as shown in Figure 6. The requested values of the width, t_1 , and the amplitude, V_1 , of the high-voltage pulse are indicated on the figure. It should be noted that the traces are offset vertically from the 250 kHz trace for ease of visualization. All the traces displayed in Figure 6 are at 25% duty cycle.

Figure 3 show that the frequency of the waveforms has little effect on CV, PWHM, or R_p . This is as expected, since the frequency of the waveform (and thus the rate of ion oscillations perpendicular to the gas flow) should not affect the CV where the ion is transmitted.

Whereas the duty cycle of the sine waveform is not variable, it is quite simple to vary the duty cycle of the square waveform. Results described below agree with the independent work conducted by Eiceman's team.⁶ At lower duty cycles (where the waveform deviates more from symmetrical) R_p increases, as

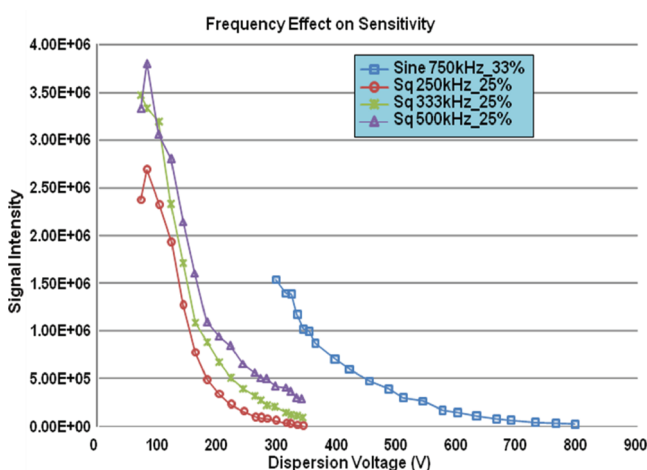


Figure 8. Graph displaying the effect of square waveform frequency on sensitivity.

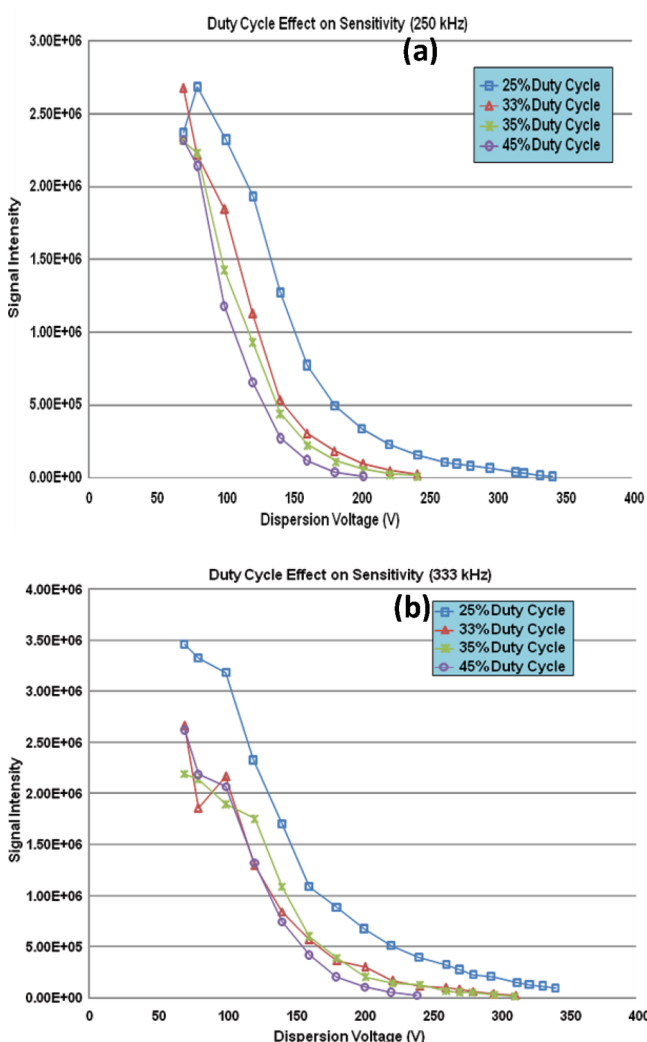


Figure 9. Graphs displaying the effect of duty cycle on sensitivity. Frequencies are 250 (a) and 333 kHz (b).

displayed in Figure 7. Note that, at 200 DV (22 Td), a 25% duty cycle yields an $R_p \sim 5\times$ higher than a 45% duty cycle. It should be

noted that the largest DV ranges were only obtainable with lower duty cycles due to the generator's limitation; this is the reason for the truncation of data as duty cycle percentage was increased.

Influence of Frequency on Sensitivity. Higher waveform frequencies are generally thought to improve ion separation in FAIMS at the expense of transmission.⁸ The frequency of the sine waveform generator is fixed. The frequency of the square waveform can be varied, but at higher frequencies, there is more distortion in the square shape of the waveform. Figure 8 displays the effect of frequency on sensitivity as a function of DV. The figure suggests that, at a given DV and as you raise the frequency, you shorten the time period and therefore you shorten the ion displacement. Thus, at a given DV fewer ions will reach the plates to get annihilated. This translates into higher transmission. It should be noted that a 25% duty cycle was selected for these graphs to be able to show 500 kHz frequency data. Higher cycles displayed the same behavior.

Influence of Duty Cycle on Sensitivity. The duty cycle is one FAIMS parameter that has not been explored extensively in the past since the duty cycle of the sine waveform (used in all commercial FAIMS systems) is fixed at 33%. In this work, the effect of duty cycle of the square waveform on sensitivity has been explored by holding the frequency at a fixed value of 250 and 333 kHz. The results shown in Figure 9 indicate that the signal intensity increases as the duty cycle decreases. Indeed, decreasing duty cycle from 45% to 25% increases the signal by a factor of 2–3. Lower duty cycles give greater sensitivity at all frequencies examined (lower duty cycles were examined with similar results).

CONCLUSION

This paper demonstrates for the first time the practical implementation of planar FAIMS utilizing rectangular waveforms in comparison with the more traditional bisinusoidal waveforms. The independent control of frequency, amplitude, and duty cycle of a computer-generated square waveform provides more complete characterization of the transmission, resolution, and separation of ions in comparison with the corresponding results obtained while using the sum-of-sines waveform. FAIMS powered by square waveform delivers better separation and resolving power as predicted with the ion trajectory simulation. The increase of the waveform's frequency was shown to increase sensitivity but had little effect on CV, peak width, and R_p . The lower the duty cycle the higher our peak area and signal intensity. Duty cycle decreases from 45% to 25% also showed a 5× increase in R_p . The square waveform provides better separation and resolving power, while leading to small losses in transmission, i.e., sensitivity. The R_p 's obtained in this research were done without the use of curtain gas or curtain plate and extremely short path length. These design choices were meant to show the capability of the digitally produced square waveform generator on a miniature planar system with the hopes of portability. Further studies should be performed to compare square and sine waveforms, with additional explosives and mixture of explosives, different cell dimensions, and different cell geometries. The major limitation of the square waveform is the limited voltage and power that can be obtained with sine waveform generators.

AUTHOR INFORMATION

Corresponding Author

*Phone: 352-392-0557. Fax: 352-392-4651. E-mail: ryost@ufl.edu.

■ ACKNOWLEDGMENT

This research was funded by the U.S. Department of Homeland Security's Science and Technology Directorate. The authors thank Mike Shepard for his guidance during the execution of the contract.

■ REFERENCES

- (1) Buryakov, I. A.; Krylov, E. V.; Nazarov, E. G.; Rasulev, U. K. *Int. J. Mass Spectrom. Ion Processes* **1993**, *128* (3), 143–148.
- (2) Purves, R. W.; Guevremont, R.; Day, S.; Pipich, C. W.; Matyjaszczyk, M. S. *Rev. Sci. Instrum.* **1998**, *69* (12), 4094–4105.
- (3) Guevremont, R. J. *Chromatogr., A* **2004**, *1058* (1–2), 3–19.
- (4) Shvartsburg, A. A.; Tang, K. Q.; Smith, R. D. *J. Am. Soc. Mass Spectrom.* **2004**, *15* (10), 1487–1498.
- (5) Purves, R. W.; Guevremont, R. *Rev. Sci. Instrum.* **1998**, *69* (12), 4094–4105.
- (6) Papanastasiou, D.; Wollnik, H.; Rico, G.; Tadjimukhamedov, F.; Mueller, W.; Eiceman, G. A. *J. Phys. Chem. A* **2008**, *112* (16), 3638–3645.
- (7) Krylov, E. V. *Instrum. Exp. Tech.* **1997**, *40* (5), 628–631.
- (8) Shvartsburg, A. A.; Tang, K.; Smith, R. D. *J. Am. Soc. Mass Spectrom.* **2005**, *16* (1), 2–12.
- (9) Krylov, E.; Nazarov, E. G. *Int. J. Mass Spectrom.* **2009**, *285*, 149–156.
- (10) Krylov, E. V.; Nazarov, E. G.; Miller, R. A. *Int. J. Mass Spectrom.* **2007**, *266*, 76–85.
- (11) Shvartsburg, A. A.; Smith, R. D. *J. Am. Soc. Mass Spectrom.* **2008**, *19* (9), 1286–1295.
- (12) Lin, S. L.; Viehland, L. A.; Mason, E. A.; Wheaton, J. H.; Bardsley, J. N. *J. Phys. B: At. Mol. Opt. Phys.* **1977**, *17*, 3567–3579.
- (13) Guevremont, R.; Purves, R. W. *Rev. Sci. Instrum.* **1999**, *70*, 1370–1384.
- (14) Manura, D. J.; Dahl, D. *SIMION User Manual*, version 8.0, Scientific Instrument Services, Inc.: Ringoes, NJ, 2007.
- (15) Tsai, C.; Prieto, M.; Kaminsky, I.; Ferran, R.; Boumsellek, S.; Yost, R. A. Comparison of Square and Sinusoidal Waveforms on a Miniaturized Planar FAIMS Cell for Explosives Detection. Proceedings of the 57th ASMS Conference, 214, Tuesday (TPH), Philadelphia, PA, June 2009.
- (16) Krylov, E. V. *Int. J. Mass Spectrom.* **2003**, *225*, 39–51.
- (17) Eiceman, G. A.; Krylov, E.; Krylova, N.; Nazarov, E. G.; Miller, R. A. *Anal. Chem.* **2004**, *76*, 4937–4944.
- (18) Matz, L. M.; Tornatore, P. S.; Hill, H. H. *Talanta* **2001**, *54* (1), 171–179.
- (19) Tam, M.; Hill, H. H. *Anal. Chem.* **2004**, *76* (10), 2741–2747.
- (20) Rokushika, S.; Hatano, H.; Baim, M. A.; Hill, H. H. *Anal. Chem.* **1985**, *57* (9), 1902–1907.
- (21) Rorrer, L. C., III; Yost, R. A. *Int. J. Mass Spectrom.* **2010**, *300*, 173–181.
- (22) Shvartsburg, A. A.; Smith, R. D. *J. Am. Soc. Mass Spectrom.* **2007**, *18*, 1672–1681.
- (23) Prasad, S.; Tang, K.; Manura, D.; Papanastasiou, D.; Smith, R. D. *Anal. Chem.* **2009**, *81* (21), 8749–8757.